

Technology for quiet optical systems in space

Robert A. Laskin and James L. Fanson

Jet Propulsion Laboratory
Pasadena, CA 91109

ABSTRACT

The Micro-precision Control/Structure Interaction (CSI) program at JPL, is chartered to develop the structures and control technology needed for sub-micron level stabilization of future optical space systems. The extreme dimensional stability required for such systems derives from the need to maintain the alignment and figure of critical optical elements to a small fraction (typically 1/20th to 1/50th) of the wavelength of detected radiation (about 0.5 micron for visible light, 0.1 micron for ultra-violet light). This $\lambda/50$ requirement is common to a broad class of optical systems including filled aperture telescopes (with monolithic or segmented primary mirrors), sparse aperture telescopes, and optical interferometers. The challenge for CSI arises when such systems become large, with spatially distributed optical elements mounted on a lightweight, flexible structure. This paper will present an overview of the approach that is being taken by JPL's CSI program to address this challenge. In particular the paper will discuss the application of CSI technology to a specific example of a future large optical space mission. Experimental demonstration of the technology on ground-based testbeds will also be presented.

1. INTRODUCTION

A number of potential future NASA missions fall into the class of large optical systems addressed by micro-precision (X) technology. Orbiting Stellar Interferometer (OSI), Next Generation Space Telescope (NGST), Imaging Interferometer (II), Precision optical Interferometer in Space (POINTS), Astrometric Imaging Telescope (AIT), Submillimeter Intermediate Mission (SMIM), Space Infrared Telescope Facility (SIRTF), and several proposed lunar-based observatories are examples. The JPL CSI program has chosen a large optical interferometer, similar to OSI, as representative of this mission class. An optical interferometer utilizes a number of distinct telescopes, each of modest aperture, whose outputs are combined in such a way as to produce an effective aperture equivalent to the largest baseline distance between telescopes. Such an instrument can be used for high resolution imaging as well as extremely precise astrometry (positional mapping of the stars). Considerable effort has been devoted to developing the design of a particular optical interferometer configuration to serve as an analytic testbed on which to explore CSI methods. This fictitious, but representative, optical system has been termed the Locus Mission Interferometer (LMI). The principal challenge presented to CSI by such an instrument is the need to maintain positional tolerances between optical elements to the order of a nanometer and to do so over a structure (that may span tens of meters). Open loop response of such a system to the expected spectrum of on-board disturbances can result in thousands of nanometers of motion in the optical elements.

The key to meeting this challenge is the CSI multi-layer architecture, an approach to the vibration attenuation problem that combines three layers of control: structural quieting, vibration isolation, and active optics compensation. Reference 1 details a preliminary CSI design for the LMI. Incorporating two layers of the multi-layer architecture, passive structural damping and relatively low bandwidth optical element articulation, the effect of on-board disturbances on the optical performance metric was shown to be reduced by more than an order of magnitude. This is, however, far short of the three to four orders of magnitude necessary to guarantee proper interferometer performance. The present paper reports on the progress that has been made, via the application of more advanced CSI methods and components, toward achieving the ambitious vibration attenuation requirements. Improvements have been made in each of the three layers of the CSI multi-layer architecture. Isolation of the primary on-board disturbance source (i.e., Hubble Space Telescope class reaction wheels) is considered, as is the effect of extending the bandwidth of the optical control loops. The passive dampers have been

augmented by the introduction of active structural control via the replacement of certain structural members with active piezoelectric members.² These active members have embedded force and displacement sensors, and may be used not only for the reduction of structural vibration but also for compensation of structural distortion caused by time varying thermal loads.

In addition to detailing the analytically demonstrated effectiveness of the CSI multi-layer architecture in treating the challenges presented by the FMI, the paper also reports on current and future experimental efforts on ground testbeds aimed at verifying this performance. These testbeds are useful in demonstrating not only CSI component hardware but also the software tools that have been used in system design and analysis. Finally, the paper discusses two proposed flight experiments whose purpose it is to demonstrate that CSI technology is space mission ready.

2. THE FOCUS MISSION INTERFEROMETER (FMI)

Future spacebased precision optical systems can be divided into two broad categories: interferometers, where spatially distributed "small" collecting apertures are combined to synthesize the performance of a single larger aperture; and filled aperture systems, which are essentially conventional telescopes that may incorporate segmented primary mirrors due to the difficulty (and inherent weight) of fabricating large monolithic mirrors. JPL has selected a representative optical interferometer (Figure 1) as the target application on which to focus its CSI technology development efforts - hence the name Focus Mission Interferometer (FMI). One of the principal reasons for selecting an optical interferometer is the stressing nature of the vibrational stability requirements that such a system demands. It is important, however, to point out that a spectrum of other precision systems (e.g., EOS instruments, SSI microgravity payloads, SIRTF, SOFIA, SMIM, lunar observatories, etc) will also benefit from the development of Micro-Precision CSI technology. The FMI is a concrete example that allows for trade offs amongst competing CSI component technologies and for quantification of the benefits that result from the application of CSI.

An optical interferometer can be used for high resolution imaging as well as extremely precise astrometry (astrometry is the mapping of stellar positions in the sky). When used for imaging, the FMI's effective baseline of 24 meters would give it roughly 10 times the resolving power of the Hubble Space Telescope. This translates into a resolution of 5 milliarcseconds. The basic layout of the FMI was inspired by the work of Mike Shao of JPL's Observational Systems Division. Dr. Shao currently has in operation, on Mount Wilson in Southern California, a ground based version of the FMI.

The optical performance of the FMI relative to its 2.5 nanometer differential pathlength stabilization requirement has been analyzed in some detail with the conclusion that vibration attenuation factors of between 1,000 and 10,000 are necessary to meet the requirement with margin. This is one of the principal challenges that CSI technology must address. Vibration attenuation alone is not sufficient, however. The need to operate well under a micron in absolute stability represents a significant challenge in its own right. In addition to exposing the severity of the performance requirements, analysis of the FMI pointed up major deficiencies in the existing capability to design and model (in an end-to-end fashion) complex optics/structure/control systems subjected to mechanical and thermal disturbances. This challenge must be met in order to make it practical to conduct quantitative design trades early in the design process and to enable simulation of system performance prior to fabrication and test. The final challenge is to demonstrate, to those entrusted with making NASA mission decisions, that CSI hardware, software, and methodologies are mature and ready for application to flight systems. The remainder of this paper is organized around illustrating, in turn, how CSI is addressing each of the major challenges posed above.

It is important to note that since the 24-meter baseline FMI was conceived in 1989, the era of "faster, better, cheaper" has overtaken NASA's plans for very ambitious future astrophysics missions. Current interferometer mission studies are focussed on OS1, a 7-meter baseline system (Figure 2), and POINTS, a 2-meter baseline system (Figure 3). Although neither of these systems is as stressing as the FMI in terms of vibration attenuation, they still demand disturbance rejection of the order of 100:1. Thus, study of the FMI remains relevant as it instructs the vibration attenuation trade offs that will also be faced by smaller instruments.

3. MEETING THE VIBRATION ATTENUATION CHALLENGE OF THE FMI

The first challenge for an FMI class optical systems is providing three to four orders of magnitude vibration attenuation. To meet this challenge, CSI has adopted an approach that entails a multi-layer architecture, with each layer responsible for providing between one and two orders of magnitude attenuation. Currently three layers - vibration isolation, active/passive structural quieting, and optical element compensation - are considered sufficient to meet the performance requirements of systems like the FMI. The idea is to intercept disturbance energy at the source (via vibration isolation), along the transmission path (via structural quieting), and at the destination (via high bandwidth optical compensation). Each layer will have a specific realization tailored to the system under consideration. For the FMI, the structural quieting layer is comprised of 25 active members whose locations and electro-mechanical impedances have been optimized to dissipate kinetic energy from the truss structure. The vibration isolation layer is similar to that implemented on the Hubble Space Telescope (HST) reaction wheels (RW's). Improved performance, over that of Hubble, is achieved by augmenting the HST's passive system with active control using voice coil actuators. The optical compensation layer consists of both tip/tilt control siderostats and fast steering mirrors as well as translation control stages to correct and stabilize optical pathlength through the system. An overall closed loop bandwidth of 2501 Hz has been simulated for the pathlength control loop, with a PZT providing the vernier high bandwidth actuation. For the vibration analysis, the disturbance source used was the imbalance force from 4 HST RW's spinning from 0 to 3000 RPM (i.e., 501 Hz).

Figure 4 shows pathlength error for the FMI's outermost interferometer as a function of RW speed. Notice that, without control, the response exceeds the 2.5 nm requirement at virtually every RW speed, and in several speed ranges exceeds 1,000 nm. In an RMS sense, the uncontrolled pathlength response is greater than 700 nm across all wheel speeds. As layers of control are added - structural quieting, vibration isolation, and pathlength control, in turn - RMS vibration attenuation factors of 5, 20, and 7 are achieved, respectively. The resultant 3-layer RMS attenuation factor of 700 means an RMS pathlength stability of just over 1 nm. In a 3-sigma sense, a worst case pathlength error of 10,000 nm is reduced by a factor of 1,000 to 10 nm.

Clearly, in the world of computer simulation, the CSI multi-layer architecture appears to be capable of meeting the three to four orders of magnitude vibration attenuation requirement. The next question is whether this conclusion holds up on actual physical systems under laboratory conditions.

4. EXPERIMENTAL DEMONSTRATION OF THE MULTI-LAYER ARCHITECTURE

To experimentally demonstrate that the CSI multi-layer architecture can meet this challenge, and prove that the successive layers are not unstably interactive, JPL has built a dedicated test facility called the CSI Phase B Multi-Layer Testbed.^{3,4} The Phase D Testbed has been built to resemble a portion of an interferometer telescope, including a laser star simulator, a metering truss structure, an optical pathlength delay line, and the associated instrumentation and real time control computers. It has proven to be an excellent setting in which to investigate the blending of the three layers of the multi-layer architecture: structural quieting, vibration isolation, and optical compensation. Figure 5 depicts the testbed and points out each layer of control. The disturbance is mounted on a single axis vibration isolation stage. The disturbance transmissibility (i.e., transfer function) from this source to optical pathlength stability (as measured by a fringe detector monitoring the laser "star simulator" signal) represents the figure of merit for experiments conducted on the testbed.

4.1. The CSI Structural Quieting layer

Lightly damped resonances in structures amplify the effects of disturbances and result in much greater levels of vibration and jitter. Structural vibration in turn causes misalignment in the optical train. Precision structures generally manifest low levels of damping because energy dissipating mechanisms such as friction are eliminated due to the precise tolerances of the joints and connections.

The CSI structural quieting layer is specifically designed to reduce the level of vibration in the structure. This is accomplished through a combination of passive damping and active control using active structural members. Passive

dampers have the advantages of simplicity of design and of requiring no power for operation. Four Honeywell 10-Strut⁵ passive dampers are installed in the Phase B Testbed (Figure 6). Active structural members, 6-11 which utilize an embedded piezoelectric or electrostrictive actuator, have the advantage of being tunable for optimal performance even after the structure has been assembled and/or deployed. The active dial-a-strut control circuit can not only be tuned to emulate passive dampers, but can also be designed to achieve a more exact impedance match to the structure, providing damping performance tailored to frequency.¹² 10-Strut⁵ designed active members are installed in the testbed (Figure 6). The active and passive members have been optimally located in the structure through the use of algorithms designed to minimize disturbance transmissibility from the disturbance source to the optical pathlength metric.¹³ 14 "The performance of the structural quieting layer, in terms of disturbance attenuation, is seen by comparing the two transfer functions depicted in Figure 7. All modes below 80 Hz exhibit damping exceeding 5% of critical, compared to damping ratios between 0.1% and 1.0% in the undamped structure. In addition to providing reduced disturbance transmission through the structure, the structural quieting layer has a stabilizing effect on the other layers of control, especially the high performance optical compensation layer. This stabilizing effect leads directly to higher bandwidth optical control, which in turn results in at least a factor of 5 improved disturbance rejection.

Recently the active member has taken a major step forward toward flight qualified status. The solid state actuator technology at the heart of the active member was flown successfully in the Actuated 10-Mirror (A10M) as part of the Hubble Recovery Mission.¹⁵ The A10M is an optical component in the new Wide Field/10-Mirror Camera (WF/PC-2) which was successfully installed in the HST by astronauts in December of 1993. The A10M uses electrostrictive actuator technology, originally developed by Litton/Itek Optical Systems for Department of Defense deformable mirror applications. Because electrostrictive actuator technology is relatively new, the HST recovery mission represents its first space flight application. The research that supported the A10M for Hubble will continue to advance the readiness of precision active members that will be effective in precision alignment and structural quieting applications. The successful flight of the A10M gives tremendous impetus for incorporation of CSI active member technology in near term flight missions.

4.2. The CSI Disturbance Isolation Layer

Vibration isolation is the first line of defense against the performance threatening effects of mechanical disturbances on-board micro-precision systems. For applications where the most significant disturbance sources (e.g., reaction wheels, tape recorders, etc) can be housed together in a single "dirty box," the vibration isolation layer, in the CSI multi-layer architecture, is likely to provide the greatest performance enhancement at the lowest cost. This is because isolation can be implemented by a single six axis device, whereas the other CSI layers (viz., structural damping and optical compensation) typically entail numerous hardware components distributed over the system. In such situations the vibration isolation layer, if sufficiently effective, will significantly relax the requirements on (if not eliminate the need for) one or both of the other layers. Thus motivated, the Micro-Precision CSI Program has recently placed increased emphasis on vibration isolation technology.

A disturbance isolation fixture was designed, built, and implemented on the JPL Phase B Testbed (Figure 8). The disturbance source was a proof-mass shaker suspended on an accordion type flexure which in turn was rigidly attached to the truss structure. The corner frequency of the soft mount was measured at 3 Hz with natural damping on the order of 12% of critical. An active stage consisting of a voice coil actuator and an LVDT displacement sensor was added in parallel with the soft mount. Active control experiments using positive position feedback (PPF) were successful in reducing the corner frequency of the isolator by a factor of 2 over the passive design. The experimental results (Figure 9) show the improvement in optical performance when the isolator is turned on. A broadband RMS attenuation factor of greater than six was achieved.

Recent improvements in isolator design have enhanced this performance by another factor of five.¹⁶ The compact single-axis device pictured in Figure 10 has demonstrated 30 dB of broadband vibration isolation (Figure 11). Plans call for building a six-axis unit consisting of six single-axis devices configured as a "Sewart Platform." In theory such a unit should be capable of fully isolating a micro-precision spacecraft from all translational and rotational disturbances. This theory will be put to the test in a proposed NASA flight experiment: the Six Axis Smart Strut Isolation Experiment (SASS)). SASS) is about to enter Phase A development with launch aboard the space shuttle planned for 1997.

4.3. The CSI Optical Compensation Layer

The optical delay line experiment was designed to capture the interaction between structural flexibility and optical pathlength as it would occur in a space-based optical interferometer such as the IM 1. '7' 18 Varying levels of control/structure interaction can be emulated by reconfiguring the testbed optical train. The configuration shown in Figure 12 represents a typical case for an interferometer, where the laser beam bounces off mirrors located on opposite ends of the truss structure. Vibrational motions of the mirrors in the path of the laser beam change the length of the optical path and this change is measured interferometrically by a fringe detector. Control of the optical pathlength is provided by a coarse motion voice coil actuator and a fine motion piezoelectric actuator.

With the testbed excited at the natural frequency of a major structural mode, closed loop experimental results indicate (Figure 13) that stellar pathlength variations were reduced from 2.4 micrometers RMS to approximately 5 nanometers RMS (the testbed noise floor). In addition, it was demonstrated that if a white noise disturbance excited the structure with energy uniformly distributed over 1--1001 Hz, the optical control layer would reject it by a factor of 139 RMS (see Figure 14).

4.4. Multi-Layer Performance on the Phase B Testbed

The multi-layer experimental results are given in terms of the disturbance transmission function from disturbance source to optical pathlength. The frequency response plot of Figure 15 summarizes the results and shows how each layer, implemented successively, lowers the disturbance transmission function. Assuming that a band-limited white noise disturbance excites the structure with energy uniformly distributed over 1--1001 Hz, the RMS attenuation factor achieved by each layer in that frequency band is: (i) structural quieting: 6; (ii) disturbance isolation: 6; (iii) optical control: 139.

With all layers operating together, the multi-layer architecture enables a **5100:1 vibration reduction**.¹⁹ Clearly, the biggest contributor to vibration attenuation performance is the optical control layer. However, the structural quieting layer was essential in enabling this level of optical compensation. Without the level of damping introduced by structural quieting, the optical control bandwidth would have been reduced by at least a factor of 3 (in order to preserve system stability), resulting in a factor of 5 - 10 poorer vibration attenuation. This recognition leads us to regard the optical compensation and structural quieting layers as essentially equal contributors (factor of 30 each) to overall vibration attenuation performance. Also of note is the achieved level of absolute optical pathlength stability in the ambient laboratory environment: **5 nanometers RMS**. The principal contributors to this residual level were fringe detector resolution (~ 2 rim), noise in the control electronics, and laboratory acoustic and seismic excitation. Since the latter two noise sources are not present in space, and the former two are readily dealt with by near term improvements in electronics design, the promise of sub-nanometer stabilization of space optics appears quite feasible.

5. INTEGRATED MODELING AND DESIGN TOOLS FOR CSI SYSTEMS

The challenges facing Micro-Precision CSI do not lie exclusively in the province of developing hardware for vibration attenuation in the sub-micron regime. Work is also needed to advance the state-of-the-art for software tools for analysis and design. Existing analysis tools provide only limited capability for evaluation of spaceborne optical system designs. They determine optical performance from the geometry and material properties of the optical elements in the system, assuming only minor deviations from the nominal alignment and figure. They cannot evaluate the impact on optical performance from controlled/articulated optics, structural dynamics, and thermal response, which are important considerations for future large optics missions. To investigate these critical relationships, a new optical system analysis tool has been developed called the Controlled Optics Modelling Package (COMP).^{20,21} It is a computer program especially designed for modelling the optical line-of-sight, surface-to-surface diffraction, and full wave front performance of optical systems that are subjected to thermal and dynamic disturbances. COMP can accommodate the most common optical elements: flat and conic mirrors and lenses, reference surfaces and focal planes, as well as some uncommon optics, such as segmented and deformable mirrors. It can be used for stand alone analysis of optical tolerances and optical performance, or to provide the optics part of an integrated system model for error analysis and budgeting, or for system calibration and cad-to-end simulation performance

analysis. Integration of COMP with emerging CSI analysis tools will make it possible to optimize the design of a combined control/structure/optics system for maximum optical performance. All of these capabilities make COMP an important new analysis tool which enables comprehensive investigations of complex optical system architectures such as those to be used for space and lunar based telescopes and interferometers. COMP has already seen application to the LMI as well as to on-going NASA flight projects including Hubble Space Telescope and SIRTIF. JPL is currently in the process of embedding COMP in a more comprehensive integrated analysis package called IMOS (Integrated Modeling of Advanced Optical Systems).²² IMOS will enable end-to-end modeling of complex optomechanical systems (including optics, controls, structural dynamics, and thermal analysis) in a single seat workstation computing environment. Version 1.0 of COMP as well as an initial version of IMOS have been completed and released, along with comprehensive User Guides. They are available through COSMIC.

The process of system design is one of synthesis. Analysis tools such as COMP and IMOS have value in this process in that they are able to quickly evaluate competing point designs. However, analysis tools in their own right do not enable direct design synthesis. The key challenge in design synthesis is performing trade off studies pitting competing objectives from differing subsystems against one another. Too often such studies are based solely on "engineering judgement" and are wholly non-quantitative in their approach. The more complex the system, the more likely this is to be the case. JPL has recently completed work on an initial set of software algorithms (the Integrated Design Tool) that enables quantitative trade offs across the structural, optical, and control subsystems.²² This design tool has been used to conduct a case study on the JPL Phase B Testbed that explores the trade-off between mass and performance in precision optical systems. The result is a family of testbed designs that would simultaneously provide improved optical performance and decreased mass. The current software is also capable of optimizations that include placement and tuning of damping elements, and the utilization of optical performance metrics such as Strehl ratio and wavefront error.^{25,26} This design optimization methodology promises to enable the generation of highly efficient, light weight, control/structure designs required to support NASA's future optical systems.

6. END-TO-END TESTING OF MICRO-PRECISION CSI TECHNOLOGY

To demonstrate the solution to the LMI-class control challenge, CSI technology evolution requires ground-based validation at the subsystem level followed by a successful demonstration of end-to-end instrument operation, first on the ground and then in space. Resulting technologies can then be applied to specific space-based interferometric missions or to other precision missions which exhibit similar challenging requirements.

6.1. The Micro-Precision Interferometer (MPI) Testbed

The Micro-Precision Interferometer (MPI) Testbed²⁷⁻²⁹ pictured in Figure 16 provides a crucial link between interferometric technologies developed for ground systems and those required for space. Its design draws upon extensive interferometer and CSI experience. The Mount Wilson Mark III Interferometer is an operational ground-based instrument capable of performing astrometric measurements.³⁰ Although overall performance is limited by the atmosphere, this facility provides a demonstration that precision alignment and control of its optical elements can be achieved when the instrument is attached to a non-flexible body such as the earth. Results from the JPL CSI Phase B Testbed, which includes a subset of the optical elements found on the Mount Wilson Mark III Interferometer, demonstrate that the required nanometer level sensing and control requirements can be achieved on a flexible structure using the CSI layered architecture.

The Micro-Precision Interferometer Testbed allows for system integration of CSI technologies with key interferometer subsystems on a flexible structure. The MPI structure is a 7m x 6.8m x 5.5m truss weighing 200 kg (estimated to be 600 kg in its final configuration with optics and control systems attached). Built primarily from aluminum components, it went from elemental form to final assembly in less than four months. Considerable effort was taken in the structure assembly process to minimize alignment errors and produce a linear structure. Three linear extension springs attached to three different points on the structure make up the structure's suspension system. This system provides about a factor of ten separation between the structure's "rigid body" and flexible body modes (the lowest of which is at about 6 Hz). At this writing the

MPI structure has been outfitted with a fully operational three tier delay line with associated laser metrology and real time control computer. Kinematically mounted optical breadboards are installed. It is to these plates that the optical pointing system components (fast steering mirrors, camera heads, fold mirrors, etc) will be mounted later this year, completing the MPI's first baseline. The testbed also has mounting hardware configured to accommodate a six axis Stewart platform type isolator, also slated for delivery later this year. As currently installed, the isolator's fixture, located in the bottom bay of the MPI tower, contains six rigid struts in place of the to-be-installed isolator.

Using a "star simulator" laser metrology system located on a floated optical bench alongside the testbed, the sensitivity of "stellar" optical pathlength (from the "star," down each arm of the interferometer, and through the delay line) to mechanical excitation originating at the isolation fixture can be investigated. Figure 17 shows the transfer function from a shaker mounted on the isolation fixture to the stellar optical pathlength with the delay line control loops off. Note the testbed's lightly damped resonances (measured in previous modal surveys to have damping on the order of 0.1 %), indicative of an extremely linear structure. Note also that, open loop, optical pathlength error exceeds 1000 nanometers per newton across a broad frequency range. By way of comparison, refer to Figure 18 for the analogous (analytically derived) transfer function for the FMI. Notice the striking similarity between the FMI and the MPI transfer functions. This, of course, is no accident. The MPI was designed to be a half scale reproduction of a "cat-armed" FMI. If there is a surprise it is that the MPI, although a considerably smaller structure, appears to be somewhat more sensitive to mechanical excitation than the FMI, perhaps indicating that analytical models of such systems err on the side of optimism in predicting system performance. This, along with a host of other issues involving hardware and software validation, will be investigated in great detail when the MPI Testbed attains full (single baseline) operational status by the end of 1994.

6.2. Flight Experiments

The MPI Testbed will go a long way toward establishing end-to-end micro-precision CSI technology readiness. However, for a handful of key components, there is no substitute for the space environment to unambiguously provide performance verification. Two examples are vibration isolation and active delay lines. For the former, testing in 1-g invariably leads to the introduction of gravity off-load mechanisms which cast doubt upon the validity of the results. Similarly for the latter, gravity plays a poorly understood role in preloading critical mechanical elements, making extrapolation from ground based to space based performance extremely difficult. Prudent risk reduction in these areas indicates that testing in space is called for. Furthermore, from a psychological point of view, the excitement and impact of a space experiment should not be underestimated. "flight proven" is a term that inspires confidence in the minds of program managers.

Two flight experiments aimed at micro-precision systems technology are currently in the planning stages under NASA's INSPIRE (In Space Technology Experiment) Program. As mentioned above, SASSIE will explore on-orbit performance of a rule-based six-axis vibration isolation system. A more ambitious experiment, the Stellar Interferometer Tracking Experiment (SITE) will demonstrate end-to-end optical interferometer performance in the space shuttle's cargo bay. SITE will contain an optical delay line and will establish the performance credentials of this component in zero gravity.

7. SUMMARY

This paper has presented a broad brush overview of the JPL Micro-precision CSI Program and the technology it is developing to enable future optical class NASA space missions. The program has been pursuing a plan that combines hardware development (components for sub-micron structural control, vibration isolation, and optical element articulation), software development (integrated analysis tools such as COMP and IMOS as well as the Integrated Design Tool), and the development of an overall system philosophy (viz., the CSI multi-layer architecture). To date, analytical results on the Focus Mission Interferometer and experimental results on the Phase B Multi-layer Testbed demonstrate the promise of micro-precision CSI technology. What remains is the demonstration of technology flight readiness via end-to-end testing on the Micro-precision Interferometer Testbed and on-orbit demonstrations on SITE and SASSIE. This should lead to wholesale insertion of CSI technology into NASA precision space systems by early in the next decade.

8. ACKNOWLEDGEMENT

This work was performed at the Jet Propulsion Laboratory, California Institute of Technology, under a contract with the National Aeronautics and Space Administration. The authors would like to thank Mark Milman, Greg Neat, John Spanos, and the entire JPL/CSI team for their fundamental contributions. It is the fruit of their intellectual and physical labor that is reported here.

9. REFERENCES

1. R. A. Laskin, A. M. San Marlin, "(ontrol/Structure System Design of a Spaceborne Optical Interferometer," AAS/AIAA Astrodynamics Specialist Conference, August 1989.
2. S. W. Sirlin, R. A. Laskin, "Sizing of Active Piezoelectric Struts for Vibration Suppression on a Space-Based Interferometer," Joint U.S./Japan Conference on Adaptive Structures, November 1990.
3. D. Eldred and M. O'Neal, "The Phase B Testbed Facility," Proceedings of the ADPA Active Materials and Adaptive Structures Conference, Alexandria, VA, November, 1991.
4. D. Eldred and M. O'Neal, "The JPL Phase B Interferometer Testbed," Proceedings of 5th NASA/DOE Control Structure Interaction Technology Conference, South Lake Tahoe, Mar '92.
5. E. Anderson, M. Trudent, J. Fanson, and J. Pauls, "Testing and Application of a Viscous Passive Damper for use in Precision Truss Structures," Proceedings of 32nd AIAA SDM Conf., pp 2795-2807, '91
6. J. Fanson, G. Blackwood, and C. Chu, "Experimental Evaluation of Active-Member Control of Precision Structures," Proceedings NASA/DOE Controls-Structure Interaction Technology 1989, NASA Conference Publication 3041, Jan 29- Feb 2, '89
7. J. Fanson, G. Blackwood, and C. Chu, "Active-Member Control of Precision Structures," Proceedings of the 30th AIAA Structures, Structural Dynamics and Materials Conference, Mobile, AL, April, '89
8. B. Wada and E. Crawley, "Adaptive Structures," *Journal of Intelligent Material Systems and Structures*, vol 1, No. 2, pp. 157-174, 1990
9. J. Fanson, E. Anderson, and D. Rapp, "Active Structures for Use in Precision Control of Large Optical Systems," *Optical Engineering*, Nov '90, Vol 29 Number 11, ISSN 0091-3286, pp. 1320-1327
10. E. Anderson, D. Moore, J. Fanson, and M. Ealey, "Development of an Active Truss Element for Control of Precision Structures," *Optical Engineering*, Nov '90, Vol 29 Number 11, ISSN 0091-3286, pp. 1333-1341
11. C. Chu, B. Lurie, and J. O'Brien, "System Identification and Structural Control on the JPL Phase B Testbed," Proceedings of 5th NASA/DOE Control Structure Interaction Technology Conference, South Lake Tahoe, Mar '92.
12. B. Lurie, J. O'Brien, S. Sirlin, and J. Fanson, "The Dial-a-Strut Controller for Structural Damping," AIAA/AAS/ASME/SPIE Conf. on Active Materials and Adaptive Structures, Alexandria VA, Nov. 5-7, '91.
13. M. Milman and C. C. Chu, "Optimization methods for passive damper placement and tuning," *J. Guidance, Control, and Dynamics*, to appear.
14. C. C. Chu and M. Milman, "Eigenvalue error analysis of viscously damped structures using a Ritz reduction method," *AIAA J.*, 30, 1992.

15. J. Fanson and M. Paley, "Articulating Fold Mirror for the Wide Field/Planetary Camera - 2," Active and Adaptive Optical Components and Systems -2, SPIE, vol 1920, Albuquerque, 1993.
16. J. Spanos, Z. Rahman and A. von Flotow, "Active Vibration Isolation on an Experimental Flexible Structure," Smart Structures and Intelligent Systems SPIE 1917-60, Albuquerque, NM, 1993.
17. J. Spanos and M. O'Neal, "Nanometer Level Optical Control on the JPL Phase B Testbed," AIAA/ASME/SPIE Conf. on Active Materials and Adaptive Structures, Alexandria VA, Nov. 5-7, 1991.
18. J. Spanos and Z. Rahman, "Optical Pathlength Control on the JPL Phase B Testbed," Proceedings of 5th NASA/DOD Control Structure Interaction Technology Conference, South Lake Tahoe, Mar '92.
19. J. Spanos, Z. Rahman, C. Chu and J. O'Brien, "Control Structure Interaction in Long Baseline Space Interferometers," 12th IFAC Symposium on Automatic Control in Aerospace, Ottobrunn, Germany, Sept. 7-11, 1992.
20. D. Redding and W. Breckenridge, "optical modeling for dynamics and control analysis," *J. Guidance, Control, and Dynamics*, 14, 1991.
21. D. Redding, B. M. Levine, J. W. Yu, and J. K. Wallace, "A hybrid ray trace and diffraction propagation code for analysis of optical systems," SPIE Opt. Eng. Conf., Los Angeles, CA, 1992.
22. H. Briggs, "Integrated modeling and design of advanced optical systems," 1992 Aerospace Design Conf., Irvine, CA, 1992.
23. M. Milman, M. Salama, R. Scheid, and J. S. Gibson, "Combined control-structural optimization," *Computational Mechanics*, 8, 1991.
24. M. Milman, M. Salama, M. Wette, and C. C. Chu, "Design optimization of the JPL Phase B testbed," 5th NASA/DOD Controls-Structures Interaction Technology Conf., Lake Tahoe, NV, 1992.
25. M. Milman and L. Needels, "Modeling and optimization of a segmented reflector telescope," SPIE Conf. on Smart Structures and Intelligent Materials, Albuquerque, NM, 1993.
26. L. Needels, B. Levine, and M. Milman, "Limits on Adaptive Optics Systems for Lightweight Space Telescopes," SPIE Conf. on Smart Structures and Intelligent Materials, Albuquerque, NM, 1993.
27. G. W. Neat, L. F. Sword, B. Hines, and R. J. Calvet, "Micro-Precision Interferometer Testbed: End-to-End System Integration of Control Structure Interaction Technologies," Proceedings of the SPIE Symposium on Opt. Aerospace, Science and Sensing, Conference on Spaceborne Interferometry, Orlando, FL, 1993.
28. L. F. Sword and T. G. Carne, "Design and Fabrication of Precision Truss Structures: Application to the Micro-Precision Interferometer Testbed," Proceedings of the SPIE Symposium on Opt. Aerospace, Science and Sensing, Conference on Spaceborne Interferometry, Orlando, FL, 1993.
29. B. Hines, "optical Design Issues for the MPITestbed for Space-Based Interferometry", Proceedings of the SPIE Symposium on Opt. Aerospace, Science and Sensing, Conference on Spaceborne Interferometry, Orlando, FL, 1993.
30. M. Shao, M. M. Colavita, B. Hines, D. H. Staelin, D. J. Lutter, K. J. Johnson, D. Mozurkewich, R. S. Simon, J. L. Hersey, J. A. Hughes and G. L. Kaplan, "Mark III Stellar Interferometer," *Astron. Astrophysics* 193, 1988 pp. 357-371.

31. G. Neat, R. Laskin, J. Regner, and A. von Holst, "Advanced Isolation/Precision Pointing Platform Testbed for Future Spacecraft Missions," 17th AAS Guidance and Control Conference, Keystone, CO, Feb. '94.

FMI CONFIGURATION

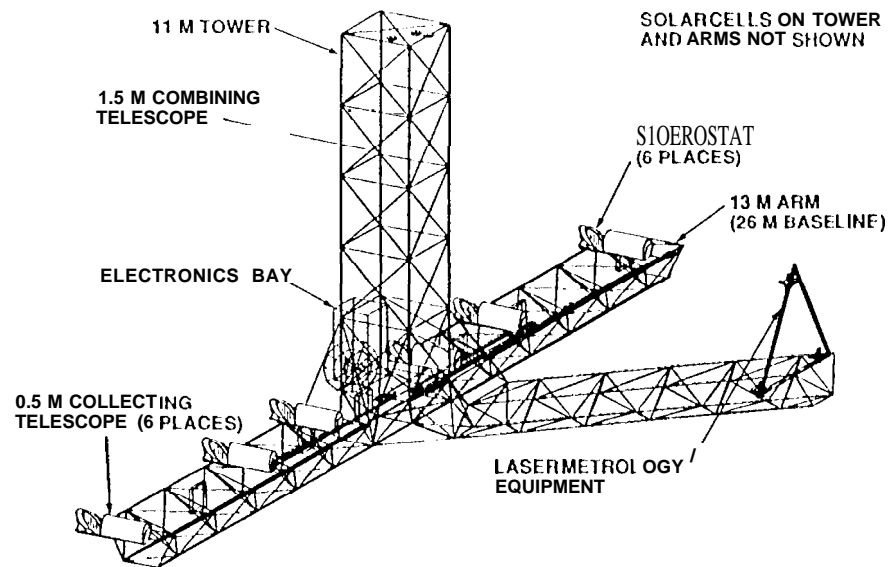


Figure 1. Focus Mission Interferometer Configuration

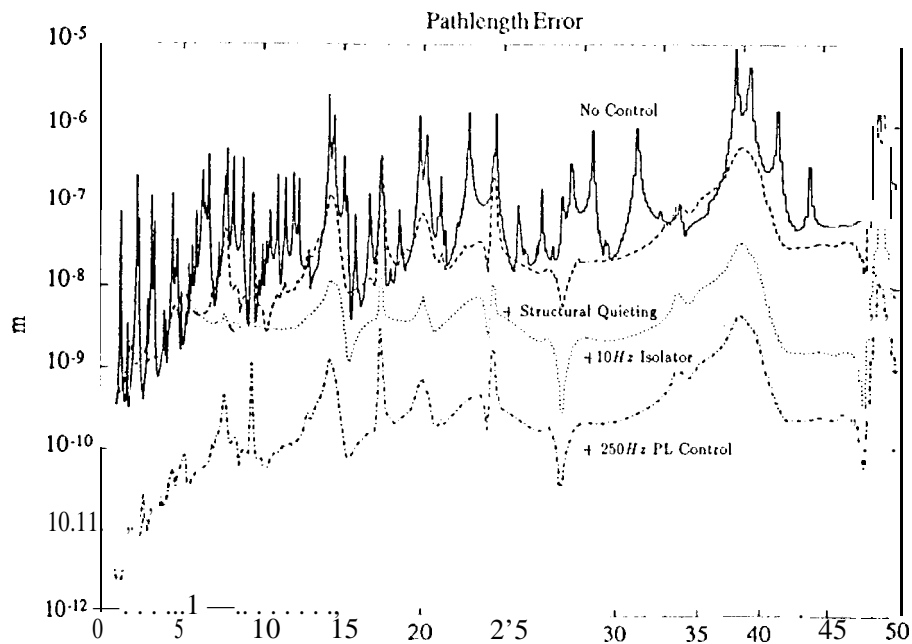


Figure 2. Optical Pathlength Control Performance on the Focus Mission Interferometer (Meters vs Reaction Wheel Speed in Hz)

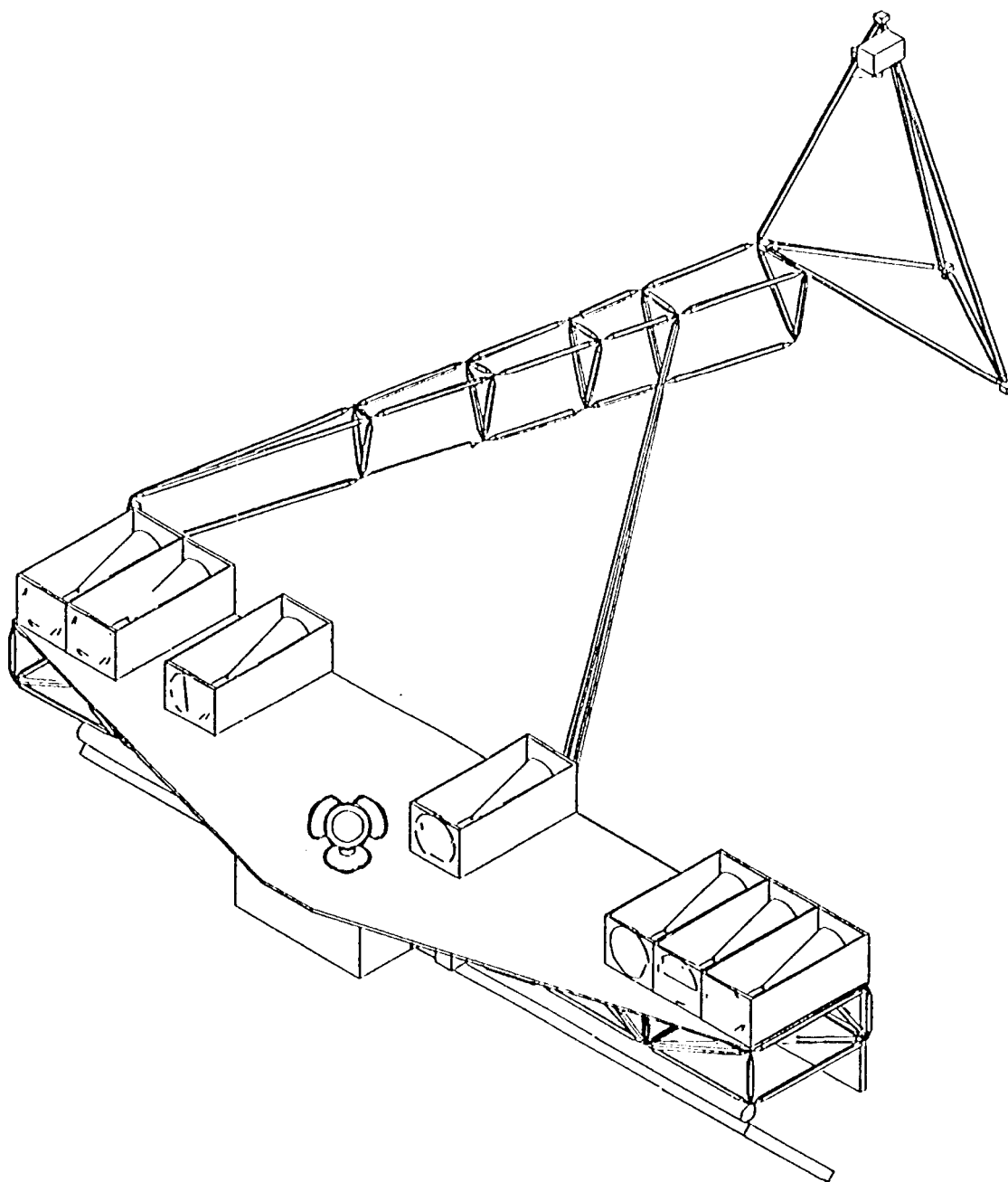


Fig 2

The Orbiting Stellar Interferometer (OSI)

mirror coatings show that about 20% of the photons entering the aperture will be detected. We find that the nominal measurement uncertainty is reached after about one minute of observing a pair of mag 10 stars. By design, the largest error component is the photon statistics of the starlight. Based on present models of slew, acquisition, and data collecting times, we estimate that POINTS would observe about 350 star pairs per day if the targets were mag 10.

Since the interferometers are mutually perpendicular, the instrument naturally performs global astrometry, which was first practiced by HIPPARCOS, and which provides three advantages: (1) Instrument bias can be routinely determined by 360 deg closure. Thus, for reasonable observing sequences, one obtains a global reference frame that is free of regional biases to the nominal accuracy of the data. (2) Parallax measurements are absolute, not relative. (3) For a given target star, the reference star is chosen from the great-circle band of sky 90 deg away, maximizing the probability of finding a suitable reference. If the relative rotation range of the two interferometers is ± 3 deg, this observable band has an area of 2160 square degrees ($>5\%$ of the sky) and can be expected to contain about 80 stars as bright as (visual) mag 5: 1200 stars, mag 7.5; and 17,000 stars, mag 10. Thus, the observation time is not dominated by the low photon rate of dim reference stars. Each reference star is a carefully studied target star, chosen from the reference grid described in Section 4.1. Thus the motions of the reference stars are well modelled and do not corrupt the measurements of other stars.

The instrument uses two kinds of metrology systems. The first is the full aperture metrology (FAM), which measures the optical path difference (OPD) in the starlight interferometers. In each interferometer, two laser gauges measure the starlight OPD and hold it fixed with respect to the "pseudobaseline" defined by a pair of "fiducial points." The second system uses these fiducial points to measure the angle between the pseudobaselines of the two starlight interferometers.

In FAM, modulated laser light is injected backward into the starlight optical path and fully illuminates the optical elements that transfer the starlight. The first element that encounters the starlight has a low-amplitude phase-contrast holographic surface. This holographic optical element (HOE) diffracts about 2% of the FAM light, and the samples of FAM light from the two sides of the interferometer are brought together to produce an error signal that drives a null servo. In the process, as discussed below, the "fiducial blocks" are surveyed into position. Each fiducial block contains four truncated retroreflectors. Constructed such that their apices coincide with the fiducial point to within a few microns. Knowledge of the six distances defined by these four points determines the angle between the pseudobaselines of the two starlight interferometers.

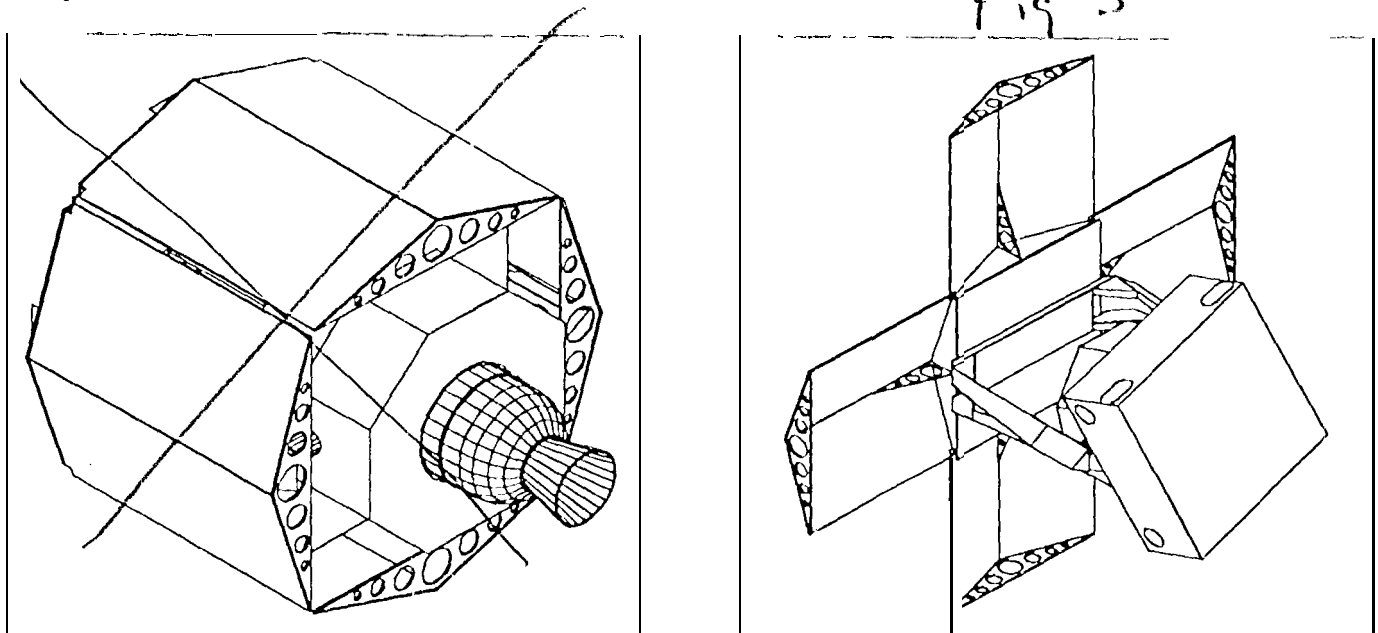


Figure 1. Proposed POINTS configuration. Left, stowed for launch. Right, operating. Not shown are four flexible triangular shields that connect the solar panels to complete the octagonal shield. *Note added in proof:* This version of the spacecraft is no longer under consideration. For the present spacecraft design, see the paper in these proceedings by Schumaker *et al.*¹⁰

JPL CSI PHASE B MULTI-LAYER TESTBED

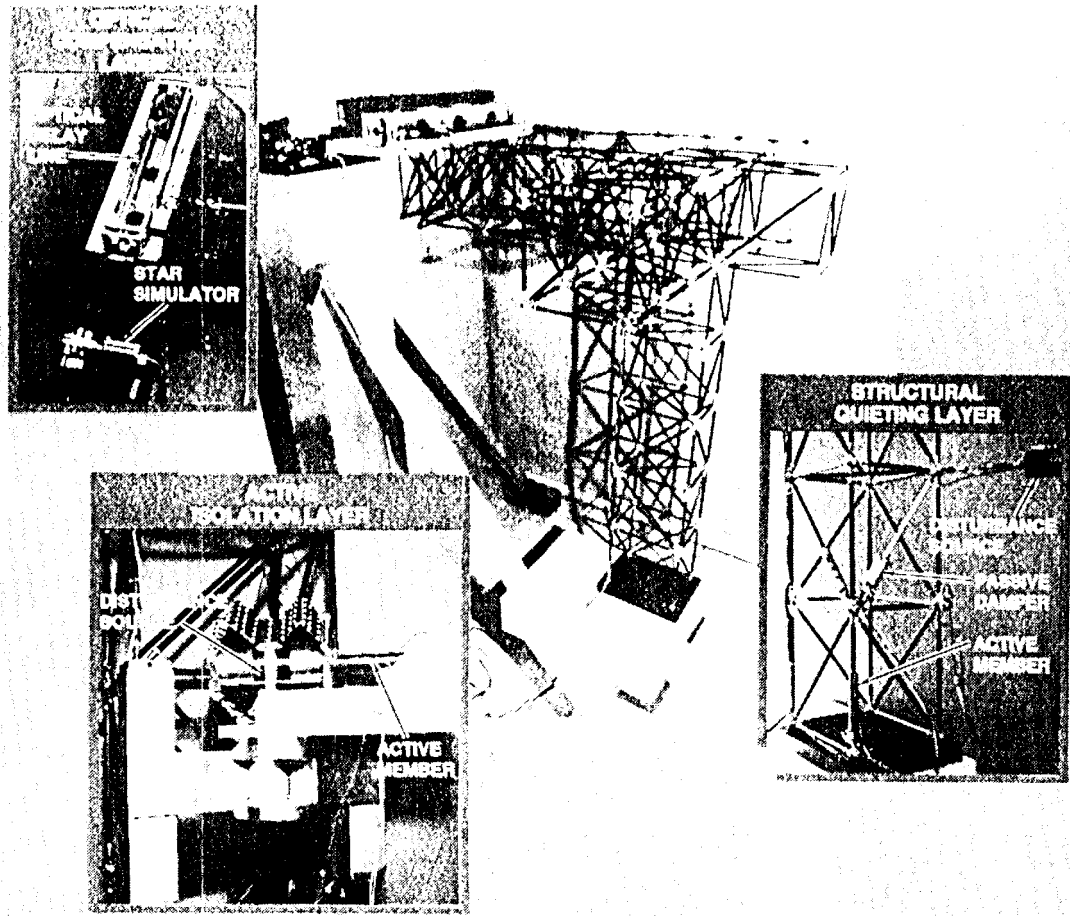


Figure 3. JPL CSI Phase B Multi-Layer Testbed

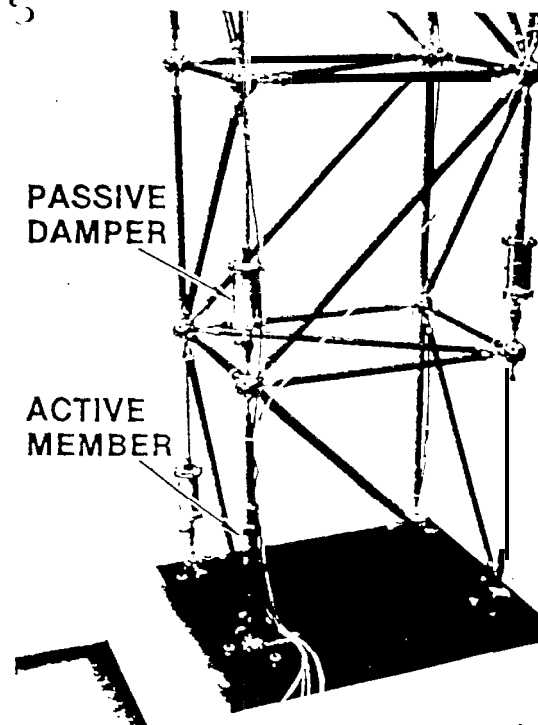


Figure 4. Structural Quieting Elements in Phase B Truss Structure

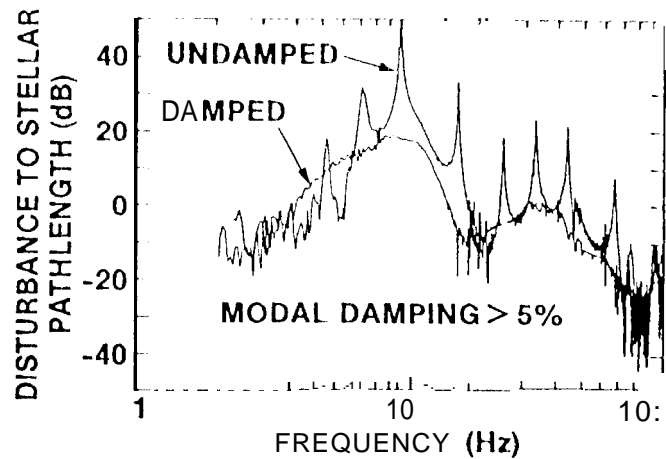


Figure 5. [Disturbance Attenuation Due to the Structural Quieting Layer

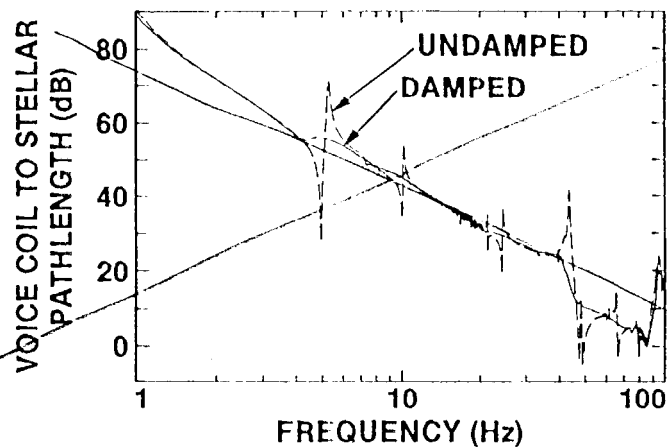


Figure 6. Frequency Response Function From Voice Coil Actuator to Optical Pathlength Sensor, Before and After Installation of Structural Quieting Layer

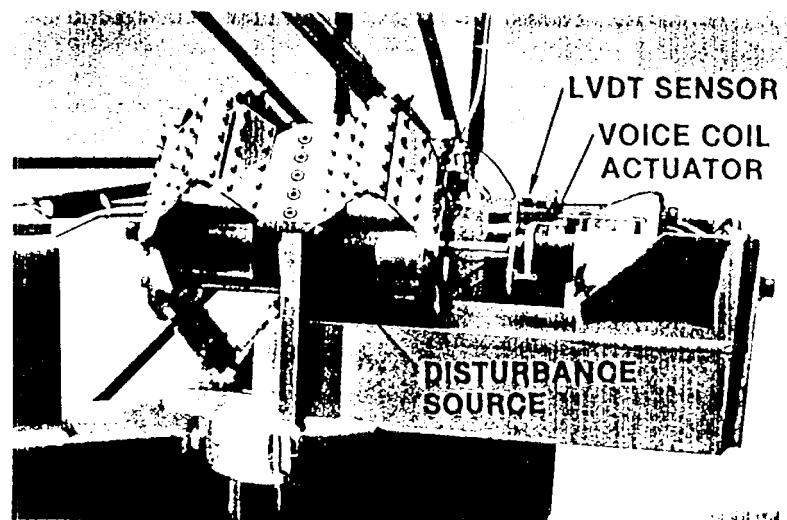


Figure 7. Phase B Testbed Disturbance Isolation Fixture

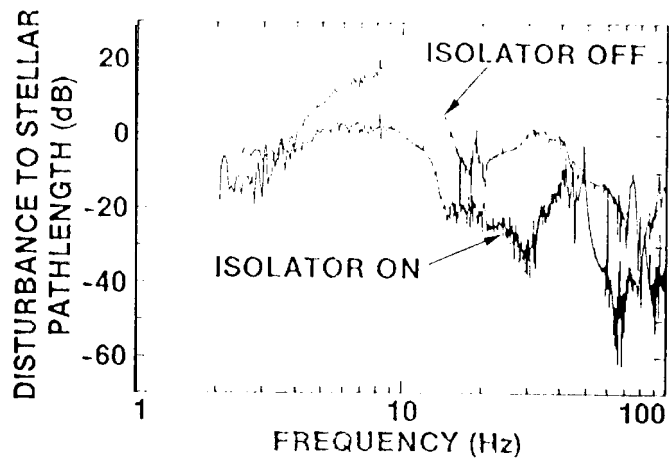


Figure 8. Disturbance Attenuation Due to the Vibration Isolation Layer

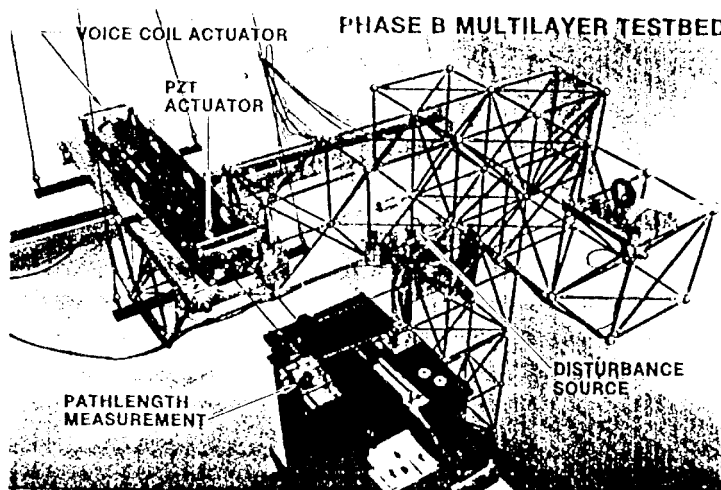


Figure 9. The Optical Compensation System on the Phase B Testbed

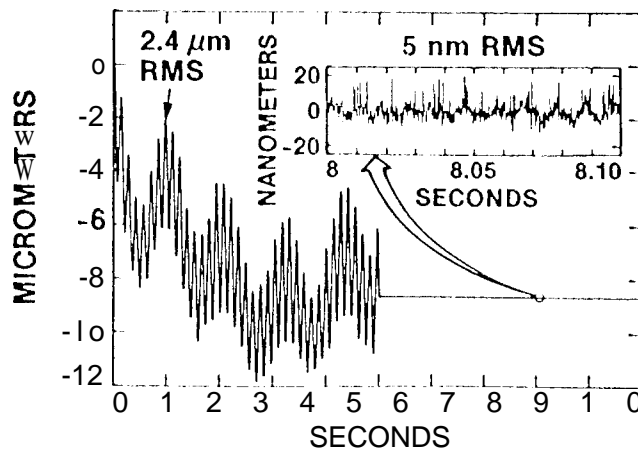


Figure 10. Optical Pathlength Response to Shaker Induced Sinusoidal Excitation -- Control Loop Closed After 5 Seconds

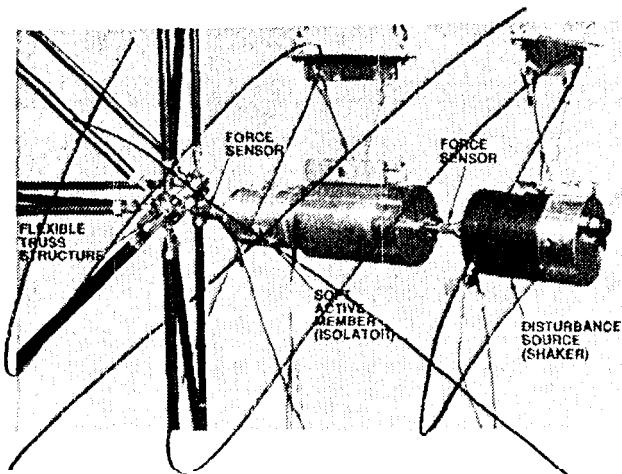


Figure 1. Vibration isolation experiment.

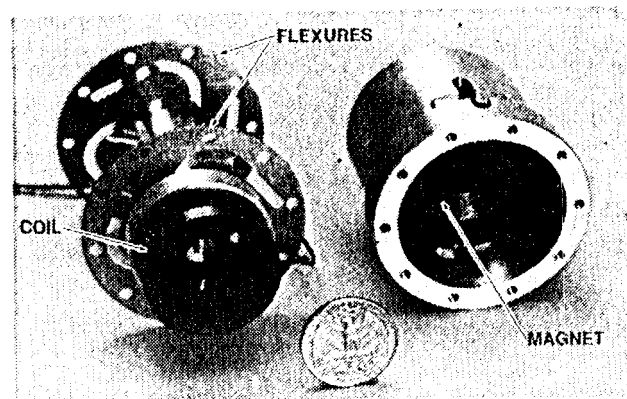


Figure 2. Soft Active Member (SAM).

The selection of actuator/sensor pairs for control has been re-examined for cases in which resonant structural dynamics are present.⁸ To summarize the results of that work:

1. A passive softmount yields not only nominal isolation performance, but also permits (with appropriate sensor/actuator pairing) decoupling of the control system from resonant structural dynamics.
2. Two actuators were identified for active enhancement of isolation; a force actuator parallel to the passive softmount, and a displacement actuator in series with the passive mount. For the force actuator, the sensor which minimized coupling with resonant structural dynamics is transmitted force. For the displacement actuator, the appropriate sensor is less constrained but still important.

This paper investigates the use of a force actuator (voice coil) in parallel with a passive softmount (elastic, flexures). The error sensor used for feedback is the force transmitted to the base. The main objective of the research is to quantitatively assess the performance gained by augmenting a passive isolator with an active control system. The work is motivated by the need to attenuate machine generated disturbances on board space vehicles but the results obtained are relevant to a large class of vibration isolation problems.

2. EXPERIMENT DESCRIPTION

A single-axis disturbance isolation fixture was designed, built, and installed on a precision truss structure known as the JPL Phase B Interferometer Testbed.⁵ The truss structure simulates an elastic foundation on which a vibrating machine is mounted. The Testbed is a highly resonant structure and early system identification tests⁹ revealed the presence of approximately 20 lightly damped modes below 100 Hz.

The experiment hardware consists of three components: the disturbance source, the isolator, and the flexible base structure. Figure 1 shows the system configuration and how the three components are interconnected along an axis perpendicular to the direction of gravity.

The disturbance source is a proof-mass shaker suspended from the ceiling and attached to the isolation fixture via a stinger-type connector. The proof mass used in the experiments was approximately 2 Kg. A force sensor was installed between the shaker and the isolator in order to measure the force acting on the isolator. This was one of two sensors used to measure force transmissibility.

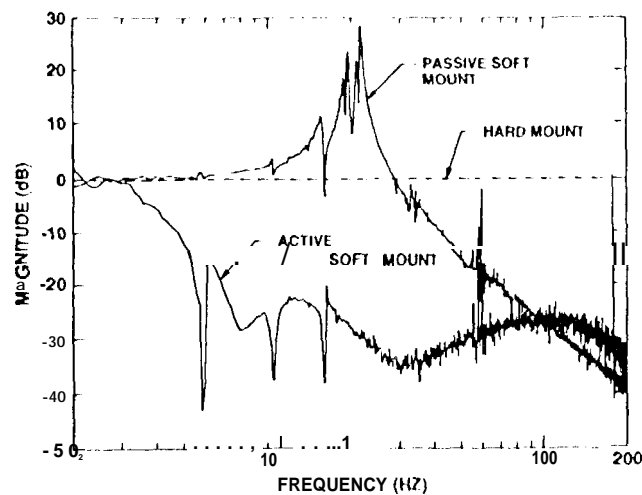


Figure 7. Isolator force transmissibility.

in the frequency domain.¹¹ The design objective was to reduce force transmissibility both below and above the passive mount corner frequency of 20 Hz. This is achieved by increasing the loop gain over the desired bandwidth. The compensator was designed to provide both broadband and narrowband performance. Loop shaping resulted in an 18th order design consisting of a second order lowpass filter, 4 second order notch filters, a fourth order lead and a fourth order lag filter. The lowpass filter provides the necessary high frequency roll-off, the lead and lag filters provide 30 degree phase margins at the high and low frequency cross-over points, and the notch filters boost the loop gain at the frequencies of the most dominant base resonances. The loop shape shown in Figure 4 shows that the compensator has introduced more than 20 dB of gain over approximately a decade of frequencies and **more than** 40 dB at select narrow bands. The design was implemented as a parallel bank of 9 second order filters on a Heurikon V3E/50MHz 68030 processor running at 4,000 Hz. The delays associated with the computer implementation (i.e., zero order hold, transport and computation] delays) were taken into account and their effects are included in the loop phase of Fig. 4.

The first experiment involved measuring the background noise in the feedback sensor. Figure 5 shows the output of the force sensor when both the disturbance source and control system are off. The laboratory background noise is on the order of 3 milli-pounds peak. The power spectrum of the waveform further shows that it is dominated by a single frequency component at 16 Hz. Since the truss structure has a lightly damped mode at 16 Hz (see Fig. 3) it is believed that laboratory ambient noise excites the 16 Hz resonance and this motion is picked up by the force sensor between the trusswork and the isolator.

Two closed loop experiments were carried out first with the ambient disturbance and then with disturbances generated by the shaker. Figure 6 shows the output of the force sensor when the feedback loop is closed. The 0.3 milli-pounds peak amplitude implies a factor of 10 improvement (20 dB) over open loop and this represents the noise floor of the experiment under closed loop control.

With the disturbance source on, the force transmissibility of the isolator was measured with and without active control. The result is shown in Figure 7. The "hard mount" represents the case of having the isolator

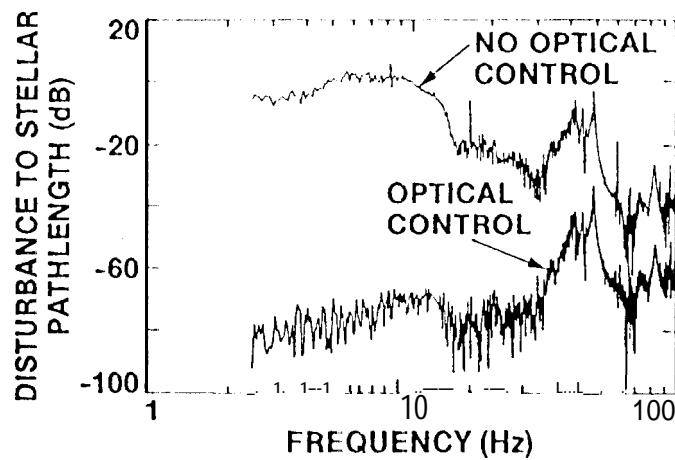


Figure 14. Disturbance Attenuation Due to the Optical Compensation Layer

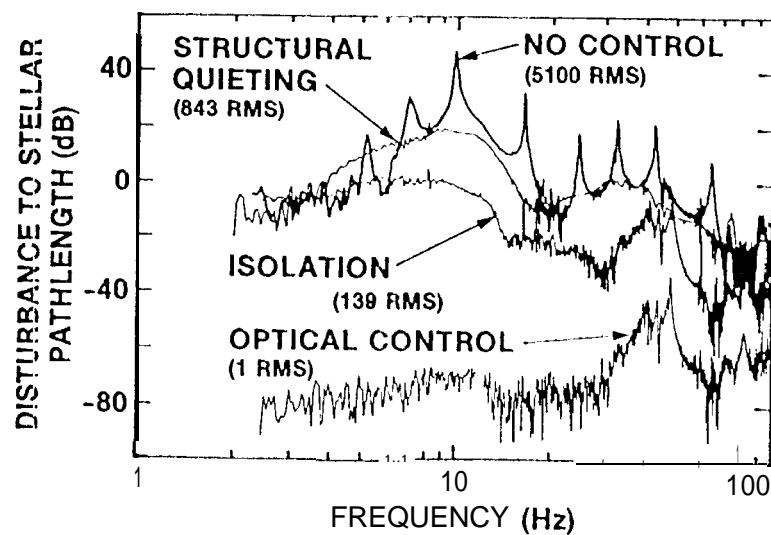
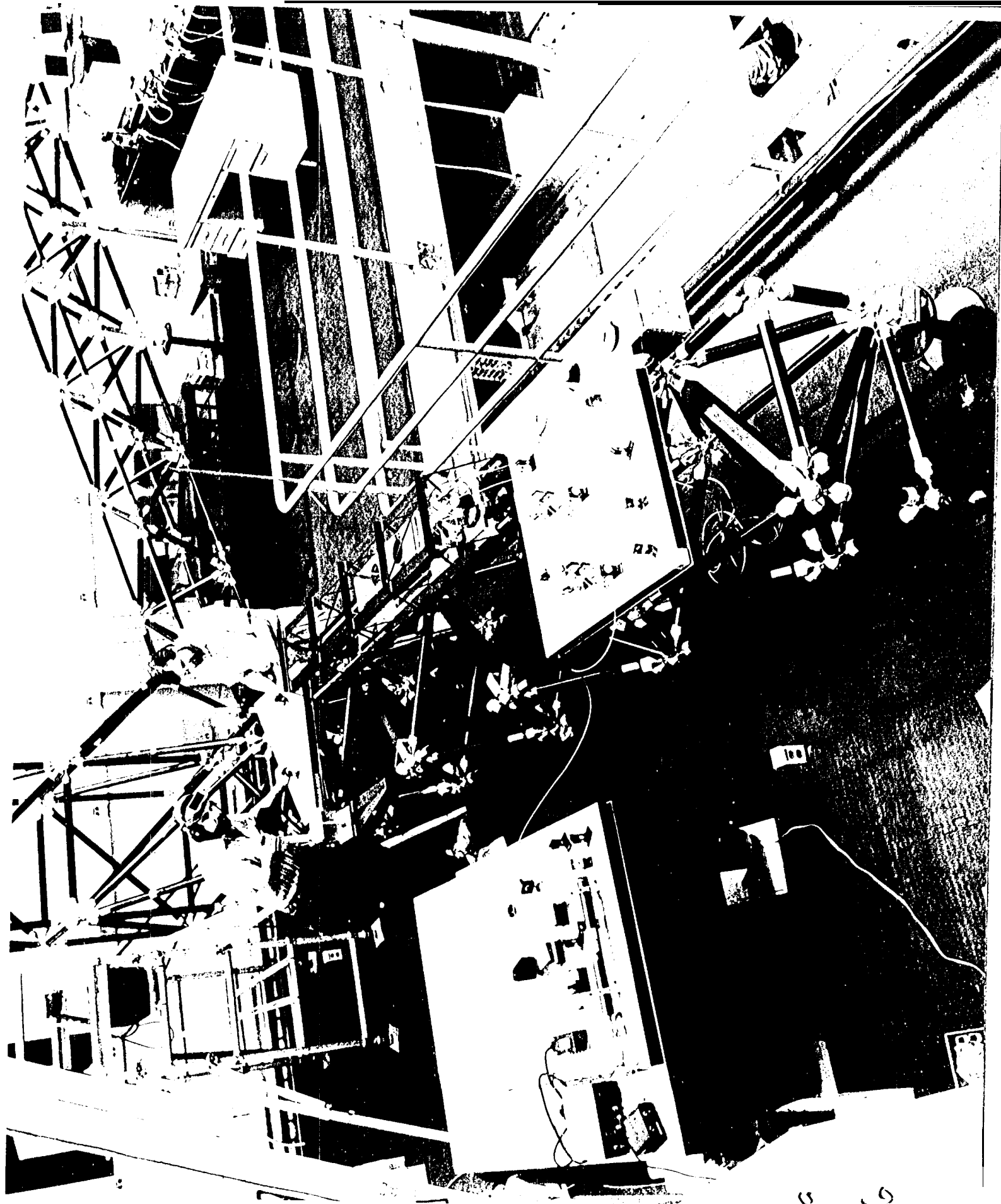


Figure 15. Disturbance Attenuation on the Phase B Testbed with All Layers Operating



11.9 1.9

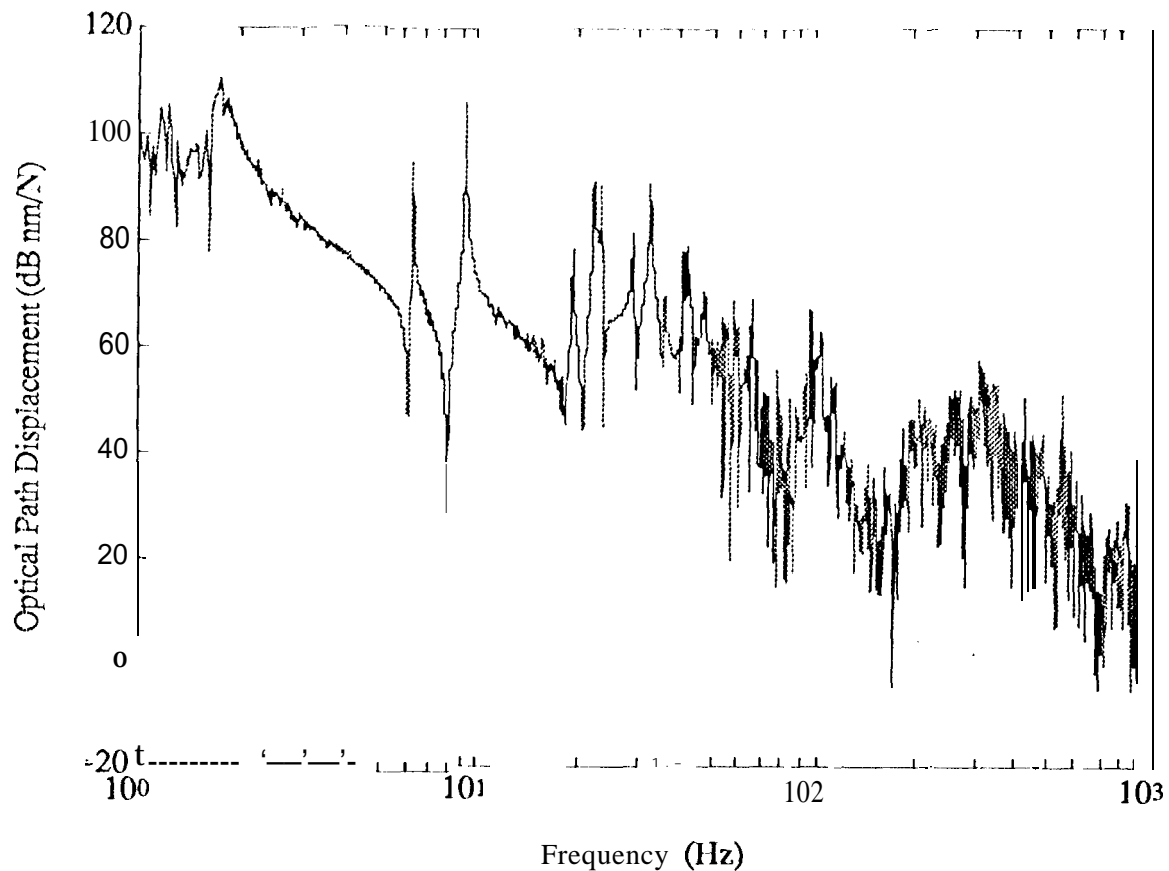


Fig. 17 Transfer function from shaker on payload plate to optical output metric.

ACKNOWLEDGMENTS

The authors would like to thank John O'Brien, Rob Calvet, Gary Blackwood, Jim Melody and Lee Sword for their help in this effort.

REFERENCES

1. G.W. Neat, L.F. Sword, B.E. Hines, and R.J. Calvet, "Micro-Precision Interferometer Testbed: End-to-End System Integration of Control Structure Interaction Technologies," *Proceedings of the SPIE Symposium on OE/Aerospace, Science and Sensing, Conference on Spaceborne Interferometry*, Orlando, FL, 1993.
2. R.A. Laskin and M. San Martin, "Control/Structure Design of a Spaceborne Optical Interferometer," *Proceedings of the AAS/AIAA Astrodynamics Specialist Conference*, Stowe, VT, 1989.
3. R.D. Reasonberg, et. al., "Microarcsec Optical astrometry: An Instrument and its Astro-physical Applications," *Astronomical Journal* 96 Nov. 1988 pp. 1731-1745.
4. M.M. Colavita, M. Shao, and M.D. Rayman, "OS1: Orbiting Stellar Interferometer for Astrometry and imaging," *Applied Optics, Williamsburg Space Optics Conference*, 1991.

Figure 59.8 freq. resp. : rw z-force dist. to patilength

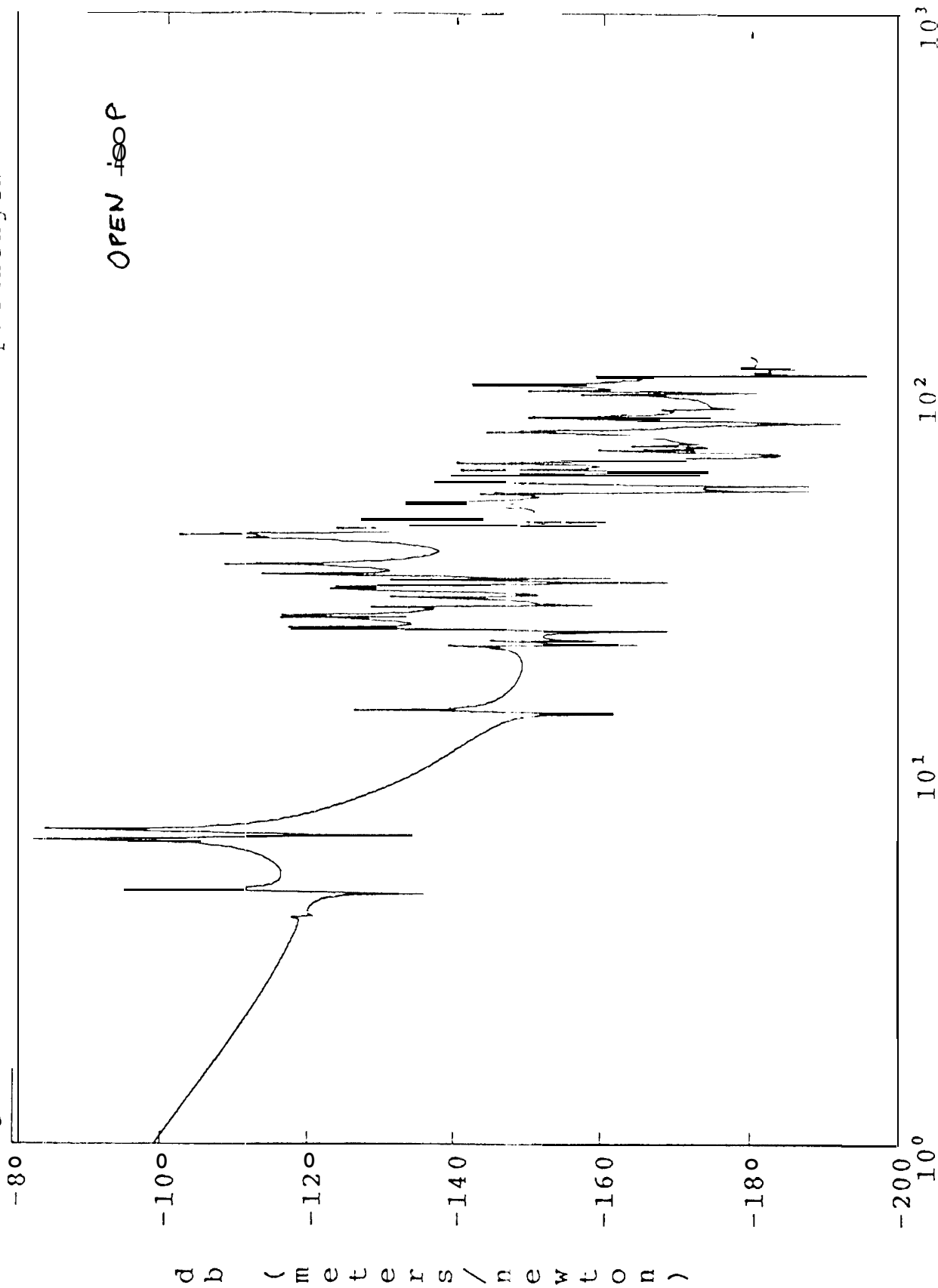


Fig 18